Hindawi Publishing Corporation
Journal of Nanomaterials
Volume 2016, Article ID 1080743, 10 pages
http://dx.doi.org/10.1155/2016/1080743

Research Article

The Synthesis of Wavelength-Controlled CdTe/Hydroxyapatite Composites and Their Fluorescence Enhancement by Bovine Serum Albumin

Li Jin,[1] Lihua Na,[2] Xueling Cao,[1] Fangli Zhong,[1] and Jianpo Zhang[1]

[1]*School of Chemical and Pharmaceutical Engineering, Jilin Institute of Chemical Technology, Jilin 132022, China*
[2]*Key Laboratory of Synthetic Rubber, Chinese Academy of Sciences, Changchun Institute of Applied Chemistry, Changchun 130022, China*

Correspondence should be addressed to Jianpo Zhang; zhangjp725@126.com

Received 4 July 2016; Revised 15 September 2016; Accepted 28 September 2016

Academic Editor: Xin Zhang

For the last ten years, quantum dots modified by biological materials have made it possible to study biochemical processes by means of biomedical imaging. This thesis introduced how the fluorescence CdTe quantum dots/hydroxyapatite composites were synthesized and how their structure, morphology, and fluorescence property were characterized by using TEM, XRD, EDS, UV-vis absorption spectra, and fluorescence spectra. The fluorescence spectra indicated the superb photometric characteristics of CdTe/HA composites. We also found that refluxing temperature and time had prominent effects on fluorescence wavelength and intensity of CdTe/HA composites, so the fluorescence emission wavelength of CdTe/HA composites could be controlled. In addition, the effect of BSA on the fluorescence properties of CdTe/HA composites was studied. The fluorescent emission intensity of CdTe/HA composites was enhanced directly with increasing concentrations of BSA; meanwhile, the fluorescence emission intensity of BSA dramatically decreased, which indicated that a Förster nonradiative energy transfer process occurred through the formation of chemical bonds between BSA and CdTe/HA composites. And the two-dimensional correlation (2D COS) was used to analyze the BSA solution before and after the reaction, which indicated that CdTe/HA composites have bound to a site at the surface of the molecule in the first subdomain IA. We also found that there was a linear relationship between the fluorescence intensity enhancement (F/F_0) of CdTe/HA composites and the concentration of the bovine serum albumin, which might become a method for quantitative analysis of BSA in a real sample.

1. Introduction

The fluorescent properties of biocompatible nanoparticles have offered attractive possibilities for medical purposes (drug and gene delivery applications) and multifunctional biological imaging to understand the biochemical processes in vitro and in vivo. Quantum dots have generated great research interest in the past two decades, due to their desirable fluorescent properties (tunable emission spectra, high photostability, resistance to photobleaching, and controllable surface characteristics, etc.) [1–9]. However, the application of quantum dots is limited, due to their characteristics of particle growth, photoinduced decomposition, biological toxicity, and conjugate aggregation [10]. Ideal biocompatible nanoparticles should have good light stability and particle size in the nanometer scale and should not be toxic for the organism. Studies have shown that the nanosized inorganic luminescent materials, as a new type of biological probes, have the potential to replace semiconductor quantum dots [11]. Among inorganic materials, hydroxyapatite (HA in short), which is the main inorganic component of animal bones and teeth [12, 13], has good biological compatibility and biological activity [14–17] and can be used as the carrier of gene, drug, and protein [18–22]. Furthermore, HA has no obvious fluorescence emission under the excitation of visible lights, which ensures that the emission spectrum of fluorescent material modified by HA is clearly observed and recorded.

Although HA has been widely used to synthesize biological luminescence materials such as La series and rare earth

ions [18, 23–27], based on the substitution of the calcium ion, there are limited reports on the synthesis of HA/CdTe quantum dots composites. Jiang et al. [28] conjugated HA derivatives (adipic acid dihydrazide modified HA, HA-ADH in short) with QDs through the reaction between amine group of HA-ADH and sulfo-NHS of QDs (QDs mixed with EDC hydrochloride and sulfo-NHS). And Li et al. [29] synthesized N-acetyl-L-cysteine-capped CdSe-polyelectrolytes @ hydroxyapatite composite microspheres through a stepwise layer-by-layer method; QDs (CdSe quantum dots) were loaded into the hollow HA microsphere, and polyelectrolyte layers were used to increase the loading amount and the electrostatic interaction between microsphere and QDs. In both researches, the HA and quantum dots were synthesized separately, and then several steps were used to conjugate quantum dots with HA. The products fabricated in this method had a diameter of several microns, and dispersion and stability depend on the precise control over conditions such as pH and ionic strength. Additionally, the N-acetyl-L-cysteine-capped CdSe-polyelectrolytes @ hydroxyapatite composite microspheres had been applied in detecting copper ion based on the fluorescence quenching of CdSe. To date, the quantum dots sensors functioned mainly through fluorescence quenching [30–35], and the synthesis of these materials with fluorescence enhancement signal has become a new challenge.

In this aspect, the coprecipitation method was used to synthesize CdTe/HA composites, and its product has bright fluorescence emission and good biocompatibility. Notably, a single light source could excite multicolor emission of different CdTe/HA composites, which clearly made them ideal candidates for simultaneous multicolor imaging in biological and medical applications. Furthermore, BSA was demonstrated as a fluorescence-enhanced reagent for the CdTe/HA composites and the mechanisms were also discussed. In addition, the fluorescent emission intensity of CdTe/HA composites (F/F_0) was enhanced linearly with increasing concentration of BSA, which suggested its great potential in real sample detection.

2. Experimental Section

2.1. Equipment. Powder X-ray diffraction (PXRD) patterns were collected on a DX-2700 X-ray diffractometer with graphite monochromatized Cu Kα radiation (λ = 0.154 nm) and 2θ ranging from 10° to 90° with an increment of 0.02° and a scanning rate of 5°/min. Absorption spectra were acquired at room temperature using a UV-2550 Shimadzu UV-VIS-NIR spectrophotometer with a 1.0 cm quartz cell. The transmission electron micrographs (TEM) were recorded with a Tecnai G220 electron microscope. The fluorescence spectra were measured on F-280 spectrofluorophotometer equipped with a xenon lamp and quartz carrier at room temperature, and the excitation and emission slit were at 2.0 nm (or 5.0 nm). The fluorescence photographs were recorded using Nikon D7000. Synchronous and asynchronous 2D correlation fluorescence spectra were taken by using Shige software.

2.2. Reagents. 3-Mercaptopropyl acid (MPA) (99+%), tellurium powder (~200 mesh, 99.8%), $CdCl_2$ (99+%), and $NaBH_4$ (99%) were purchased from Aldrich Chemical Co. BSA was purchased from Shanghai Biotechnology Co., Ltd. BSA powder was dissolved in a 2 mmol/L phosphate buffered saline solution (PBS, pH = 7.4) to obtain 1 mg/mL solution and all the solutions were stored at 0–4°C and diluted only prior to their immediate use. All other agents were of analytical reagent grade and used as they were received. Water used throughout the test was doubly distilled water (>18 MΩ·cm).

2.3. Preparation of CdTe Presoma. CdTe presoma was prepared as described in previous papers [36–38]. In brief, freshly prepared NaHTe solution, produced by reaction of $NaBH_4$ solution with tellurium powder at a molar ratio of 2 : 1, was added to nitrogen-saturated 1.25×10^{-3} mol/L $CdCl_2$ aqueous solution at pH = 11.4 in the presence of MPA as a stabilizing agent. The solutions were stirred for another 20 min and stored at 0–4°C.

2.4. The Preparation of CdTe/HA Composites. 0.3998 g $CaCl_2 \cdot 2H_2O$ was dissolved in 100 mL distilled water, the pH value was adjusted to about 10 using 0.1 mol/L NaOH, and 10 mL $Na_2HPO_4 \cdot 12H_2O$ solution (6.071 g/mL) was slowly added to the flask; this suspended precipitation was stirred for 0.5 h. Then, CdTe presoma was added to the solution, and the resulting mixture was then subjected to refluxing (80°C) under different refluxing conditions. After filtrating in pumping filtration and drying at 80°C, orange power was obtained.

2.5. Interaction of BSA and CdTe/HA Composites. 1 mg CdTe/HA composites power was dissolved in 4 mL PBS buffer solution, and pH was adjusted to 7.4. Then, a series of different volumes of 50.8 g/L BSA solutions were added to the solution. The fluorescence spectra of the resulting solutions were taken, after incubation for 10 min at room temperature.

3. Results and Discussion

3.1. Characterization of Composites. The CdTe/HA composites were synthesized using an inorganic synthesis method. As the charge and radius of cadmium ions are similar to those of calcium ions, cadmium ion along with 3-mercaptopropyl acid and NaHTe could be precipitated along with the formation of hydroxyapatite. The fluorescence intensity of CdTe/HA composites did not decrease as the temperature increased, which indicated that the CdTe quantum dots and HA were not simple physical adsorption but surface complexation and ion exchange adsorption through the formation of stable chemical bond.

Firstly, the product was characterized by TEM and XRD. As shown in Figure 1(a), the CdTe/HA composites were well dispersed on the substrate and had rod shapes with average width of about 5 nm and lengths of about 80 nm. Figure 1(b) shows that the lattice fringes of CdTe quantum dots had circular shapes with ~5 nm diameter, which overlap with the lattice fringes of HA. Figure 1(c) shows the lattice fringes of CdTe/HA composites, which indicated that introducing

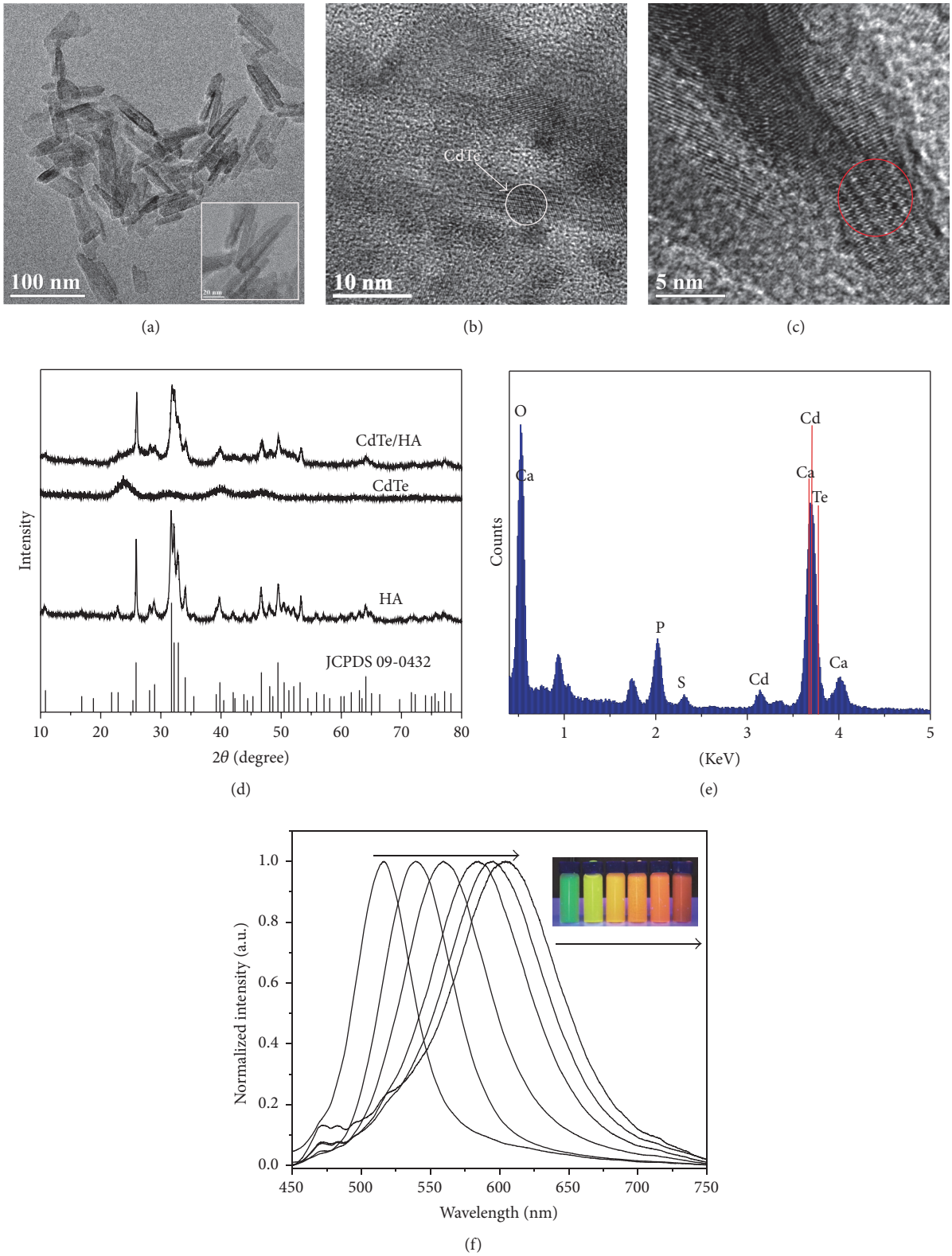

Figure 1: TEM image of CdTe/HA composites (a, b, and c); XRD pattern of HA, CdTe, and CdTe/HA composites (d); EDS spectrum of the CdTe/HA composites (e); the fluorescence emission spectra of six distinguishable CdTe/HA composites and their fluorescent photograph excited with a near-UV (365 nm) lamp (f).

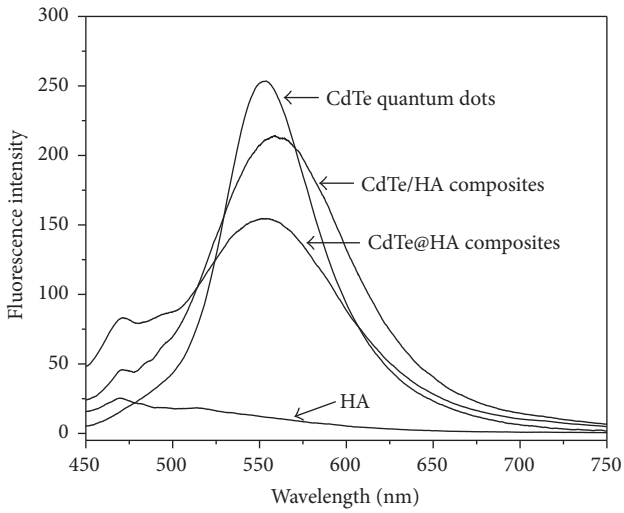

Figure 2: Fluorescence spectra of HA, CdTe quantum dots, CdTe@HA composites, and CdTe/HA composites.

CdTe did cause little lattice distortions of the HA. Figure 1(d) shows the XRD pattern of HA, CdTe, and CdTe/HA composites. HA synthesized without CdTe under the same experimental condition was used as a control. When compared with the standard data, all of the characteristic diffraction peaks could be indexed to hexagonal HA with diffraction peaks at 2θ = 25.8, 31.7, 39.6, 46.7, 49.6, and 53.2° (JCPDS number 09-0432), and no other phases could be detected. Figure 1(d) also illustrates a typical XRD pattern of CdTe prepared by a hydrothermal method, which could be indexed to the cubic structure of CdTe (JCPDS card: 01-075-2086). Due to the larger proportion of HA on the surface of the final products, the diffraction peaks of CdTe could hardly be found in XRD pattern of CdTe/HA composites. Also, EDS of the final product indicates the existence of Ca, P, O, S, Cd, and Te, confirming the detectable levels of ions within the CdTe/HA composites (see Figure 1(e)). Figure 1(f) shows the fluorescence spectra of 6 distinguishable CdTe/HA composites; from left to right (green to red), the emission maxima are located at 516, 539, 559, 583, 594, and 606 nm. The figure in the inset shows that these 6 distinguishable fluorescence emission colors observed from CdTe/HA composites are excited with a near-UV (365 nm) lamp.

Although HA alone could adsorb CdTe quantum dots due to a physical adsorption process, the adsorption amount is very limited and the interaction between HA and QDs is weak. The CdTe quantum dots (prepared by a hydrothermal method) were adsorbed directly on the HA (designated as CdTe@HA composites) for comparison purpose. The fluorescence spectra observed from different samples are shown in Figure 2. Compared with CdTe@HA composites, the CdTe/HA composites exhibit much higher fluorescence intensity, indicating increased loading amount. A rough calculation according to fluorescence intensity at 552 nm suggested that the loading amount could be increased by w37%. And the CdTe/HA composites power appeared to be fairly stable over time; when exposed to air for more than 2 months, the fluorescence intensity remained unchanged. Also, fluorescence emission intensity of CdTe/HA composites solution was measured, but no significant fluorescent quenching was observed during a period of 2 h. We assumed that the HA shell had a dramatic effect on the stability of luminescent properties compared with crude CdTe quantum dots. However, fluorescence emission intensity of this material showed significant degradation after 3 months, which showed improved resistance to air oxidation compared with crude CdTe. Furthermore, from Figure 2, we also found that there was an increase of half peak width and a decrease of the fluorescence intensities of CdTe/HA composites compared with crude CdTe quantum dots in an aqueous solution. This was probably because of the aggregation of CdTe quantum dots during the coprecipitation process. Nevertheless, the HA shell prevented flocculation and kept the structural integrity of the CdTe cores and was sufficient for fluorescent stability.

The influences of refluxing temperature and time on the peak positions and fluorescence intensity are illustrated in Figure 3. When refluxing temperature is 60°C (Figure 3(a)), the growth rate is very slow. Even after refluxing for 6 h, the peak positions of CdTe/HA composites just carry out 11 nm red shift, but fluorescence intensity increases dramatically. When refluxing temperature is 80°C (Figure 3(b)), the growth rate is faster than that at 60°C. After refluxing for 6 h, the peak positions of CdTe/HA composites carry out 60 nm red shift, but fluorescence intensity increases first and then decreases. When refluxing temperature is 100°C (Figure 3(c)), the growth rate of CdTe/HA composites is faster than that at 80°C; after refluxing for 3 h, the peak positions of CdTe/HA composites carry out about 100 nm red shift, and the fluorescence intensity also increases first and then decreases. We realized that, for synthesis of CdTe/HA composites, refluxing temperature could play a very important role in the peak positions and fluorescence intensity of CdTe/HA composites: the higher the refluxing temperature was, the longer the fluorescent emission wavelengths will be. This also indicated that the crystal size and growth rate of CdTe (growing in/on the HA) synthesized at higher temperature were larger and faster than those at lower temperature [39]. Therefore, only by varying the refluxing temperature could we control the growth rate of CdTe/HA composites, and by varying the refluxing time we could control the fluorescence emission wavelength of CdTe/HA composites in this reaction system. Note that the half band width changed markedly over time, which suggested that defocusing of size distribution takes place earlier at higher growth temperature. But when refluxing temperature was 100°C, it was difficult to control the morphology of as-prepared CdTe/HA composite. So, refluxing temperature of 80°C was employed for all subsequent studies to obtain different emission wavelength products.

3.2. The Effect of BSA on the Fluorescence Spectrum of CdTe/HA Composites. There are sulfhydryls on the surface of BSA; sulfur and tellurium (tellurium is one of the metal elements in the CdTe quantum dots) belong to the same main group, which have similar chemical properties, so sulfur could combine with cadmium on the surface of CdTe quantum dots through a chemical bond. So, we studied the effect of

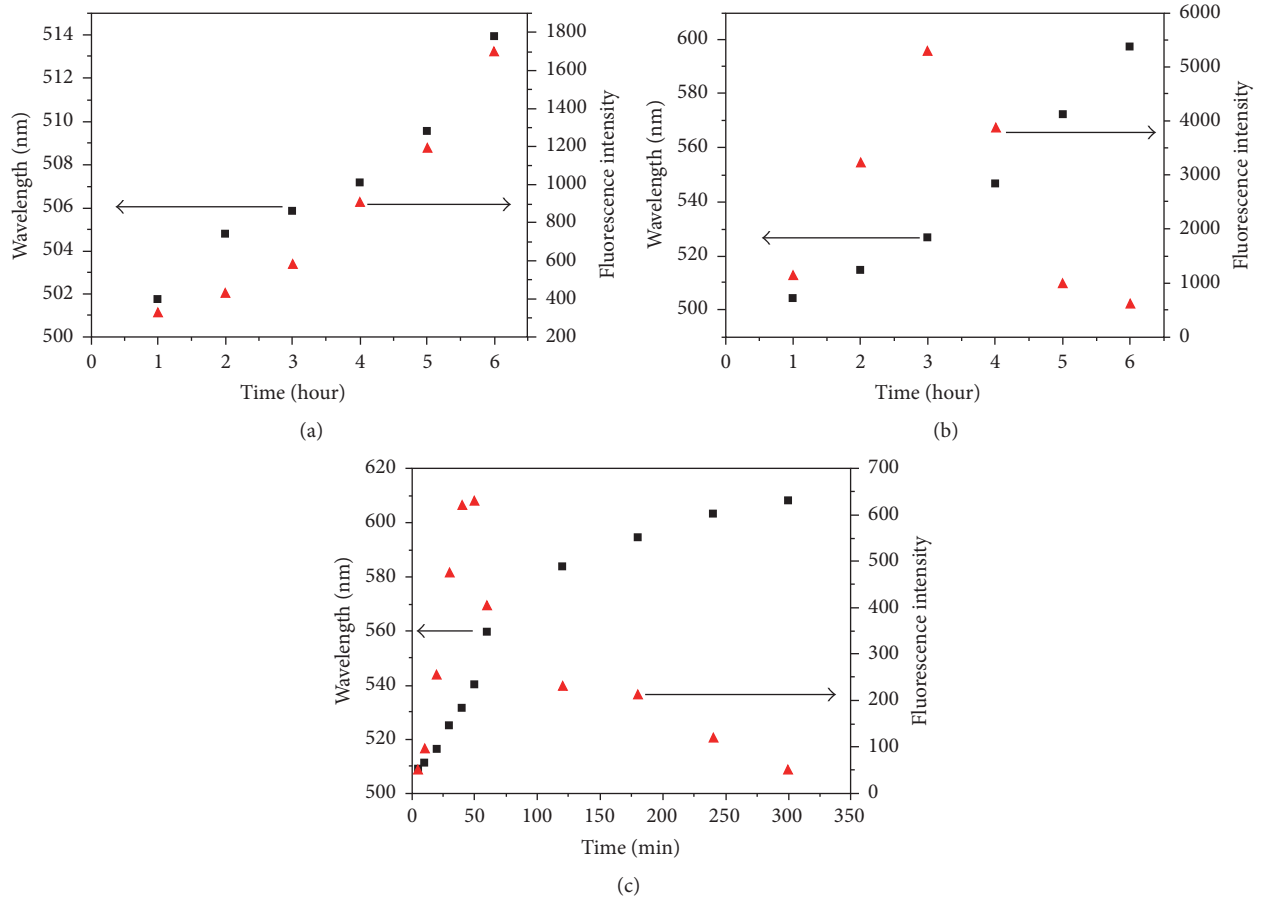

Figure 3: The effects of heating temperature on the wavelength (red triangle) and fluorescence intensity of CdTe/HA composites (black square) (temperatures of (a) 60°C, (b) 80°C, and (c) 100°C).

BSA on the fluorescence intensity of as-prepared CdTe/HA composites. Interestingly, fluorescence emission of CdTe/HA composites was enhanced obviously in the presence of BSA. As reaction requires time to be consummated, an equilibrium time of 10 min was employed for all subsequent studies to obtain consistent results. And it is well known that QDs are pH sensitive [40]; the following experiments were carried out in PBS buffer solution (pH = 7.4).

We then investigated the concentration-dependent fluorescence enhancement of CdTe/HA composites in the presence of BSA. As shown in Figure 4(a), the fluorescence emission of the CdTe/HA composites is reduced slightly at first and then is enhanced with increasing BSA concentration (as stated in the literature [41], a similar phenomenon of fluorescence-enhanced sensor has been reported). Figure 4(b) shows that the fluorescence emission intensity of CdTe/HA composites is enhanced directly with increasing quantities of BSA. Furthermore, the intensity increased (F/F_0) almost linearly against the concentrations of BSA over a concentration range from 0.05 g/L to 0.45 g/L ($R = 0.9906$) (Figure 4(c)), which could be used for quantitative analysis of BSA. The equation [30, 42] LOD = ($3.3\sigma/k$) is used to calculate the limit of detection (LOD), where σ is the standard deviation of the y-intercepts of the regression lines and (k) is the slope of the calibration graph. Here, the LOD of 0.25 mg/mL for BSA determination is 0.032 g/L. Although this method shows no advantage in linear range and the limit of detection, we do provide a new and simple method for quantitative analysis of BSA, and more detailed research will be done in the future.

3.3. Fluorescence Changing Mechanisms of CdTe/HA Composites and BSA. In addition, we measured the UV-vis spectra of CdTe/HA composites with and without BSA (Figure 5(a)). Distinctly, compared with the maximum absorption spectrum of BSA and pure CdTe/HA composites, besides the characteristic band of BSA at about 280 nm, a new band at 404 nm could be observed, implying the absorption of BSA onto CdTe/HA composites. Note there is an appreciable spectral overlap between the emission spectrum of BSA and the UV absorption spectrum (or the excitation spectrum) of CdTe/HA composites (as shown in Figure 6), and the fluorescence intensity of BSA decreases (Figure 5(b)) with the enhancement of the fluorescence emission of the CdTe/HA composites. All these meet the requirement for FRET, so we supposed that a Förster nonradiative energy transfer (FRET) process occurred through chemical interaction between BSA

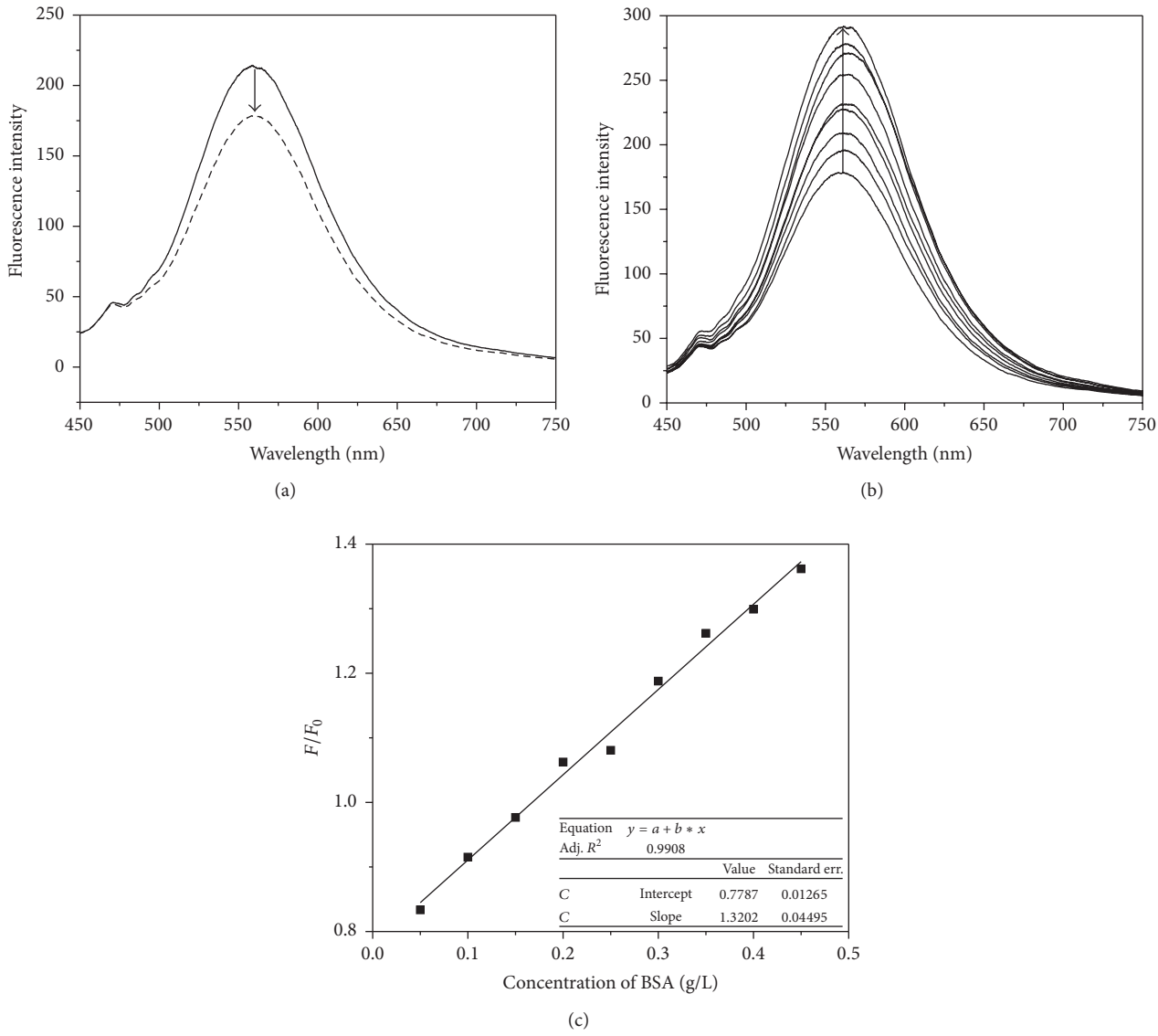

Figure 4: Fluorescence emission spectra of CdTe/HA composites (0.25 mg/mL) measured with (solid line) and without (dash line, 0.05 g/L BSA) BSA solution (a). Fluorescence emission spectra of CdTe/HA composites (0.25 mg/mL) with different amounts of BSA (0.05 g/L, 0.1 g/L, 0.15 g/L, 0.2 g/L, 0.25 g/L, 0.3 g/L, 0.35 g/L, 0.4 g/L, and 0.45 g/L); an excitation wavelength of 380 nm was used for all samples (b). The relationship between concentrations of BSA and F/F_0 (c).

and CdTe/HA composites. The efficiency (E) of energy transfer between the donor (BSA) and the acceptor (CdTe/HA composites) can be measured experimentally and calculated by (1) [43], where r is the distance between the donor and acceptor and R_0 is the donor-acceptor distance at 50%:

$$E = 1 - \frac{F}{F_0} = \frac{{R_0}^6}{{R_0}^6 + r^6}, \quad (1)$$

$$R_0 = 0.211 \left(k^2 \eta^{-4} \phi_D J(\lambda)\right)^{1/6} \ (\text{in Å}). \quad (2)$$

R_0 could be calculated by (2), where $\eta = 1.336$ is the refractive index of the medium, $k^2 = 2/3$ is the orientation factor, and $\phi_D = 0.13$ is the quantum yield of the donor in the absence of the acceptor. The spectral overlap integral $J(\lambda)$ between acceptor emission spectrum and donor absorbance spectrum was approximately calculated by origin software. In this study, we calculated $E = 0.9709$, $R_0 = 4.775$ nm, $r = 3.080$ nm, and $J(\lambda) = 5.94 \times 10^{15}$ cm^{-1}·nm^4. The values of R_0 and r were on the 2–8 nm scale and $0.5R_0 < r < 1.5R_0$. The value for R_0 was less than 5.0 nm, which indicates that efficient energy transfer takes place between the donor-acceptor pair [44]. According to the prediction of the Förster nonradiative energy transfer theory, these results indicate that the energy transfer between BSA and CdTe/HA composites could occur with high probability, resulting in the fluorescence quenching of BSA and fluorescence enhancement of CdTe/HA composites.

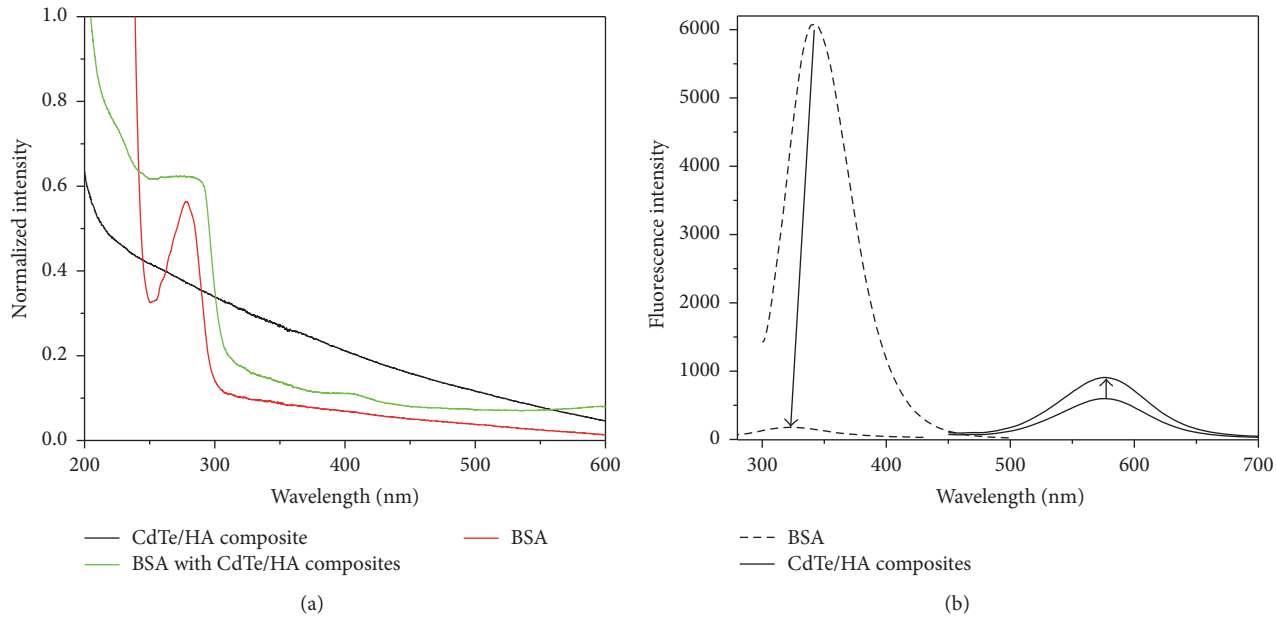

FIGURE 5: UV-vis absorption spectra of BSA, CdTe/HA composites, and BSA with CdTe/HA composites (a). The fluorescence emission spectra of BSA and CdTe/HA composites (λ_{ex} = 280 nm) (b).

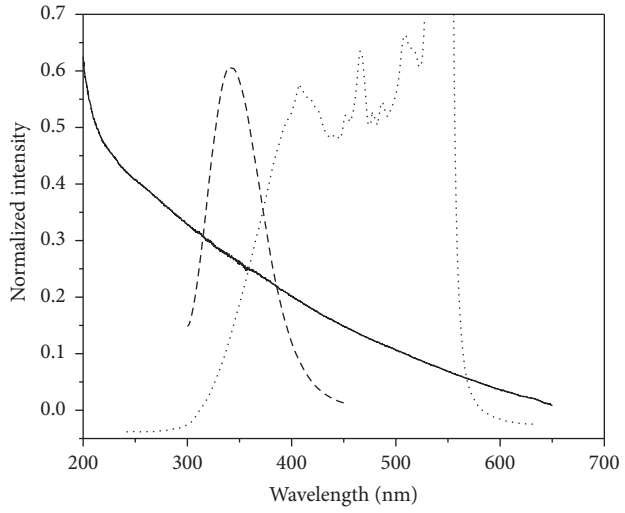

FIGURE 6: UV absorption spectra of CdTe/HA composites (solid line), the fluorescence emission spectra of BSA (dash line, λ_{ex} = 280 nm), and the excitation spectrum of CdTe/HA composites (dot line).

Meanwhile, we found that the quenching extent of the fluorescence intensity of BSA is not in proportion to the enhancing of CdTe/HA composites. It is apparent that other types of quenching mode, in addition to FRET, need to be considered as contributing factors in the quenching of the BSA emission. The 2D correlation technique was introduced to explore the quenching mechanism (as shown in Figure 7). Synchronous and asynchronous 2D correlation fluorescence spectra of pure BSA (as shown in Figures 7(a) and 7(b)) and BSA with CdTe/HA composites (as shown in Figures 7(c) and 7(d)) in aqueous solutions were constructed from the fluorescence spectra in Figure 8.

Bovine serum albumin (BSA) is composed of three kinds of intrinsic fluorophores (tryptophan, tyrosine, and phenylalanine) [43] and contains two tryptophans (Trp-212 and Trp-134) [45, 46]. It is able to assign the peak at 360 nm to Trp-134, while the peak at 325 nm is assigned to Trp-212. Because Trp-134 is located at a more polar site of the protein, the emission peak is at longer wavelength [47]. Upon excitation at 280 nm, for pure BSA solution, only one peak at (341, 341) in the synchronous correlation map (Figure 7(a)) and two distinct peaks at (325, 360) nm in the asynchronous correlation map (Figure 7(b)) were observed, respectively. So, we can conclude that the fluorescence emission peak at 341 nm is the cocontribution of the two tryptophans involved, and the overlapped peaks of the two Trp residues can be distinguished by the 2D correlation technique. For BSA and CdTe/HA composites mixed solution, only one peak at (325, 325) was observed in the synchronous correlation map (Figure 7(c)) and the asynchronous correlation map (Figure 7(d)), respectively. The fluorescence emission of Trp-134 should be quenched when BSA was added to CdTe/HA composites solution and indicated that CdTe/HA composites were bound to a site at the surface of the molecule in the first subdomain IA, close to the Trp-134. More in-depth discussion of the mechanism of the binding between BSA and CdTe/HA composites should be adopted in the future.

4. Conclusions

We have suggested a new and simple method for the synthesis of CdTe/HA composites. In particular, by varying the refluxing temperature, we could control the growth rate

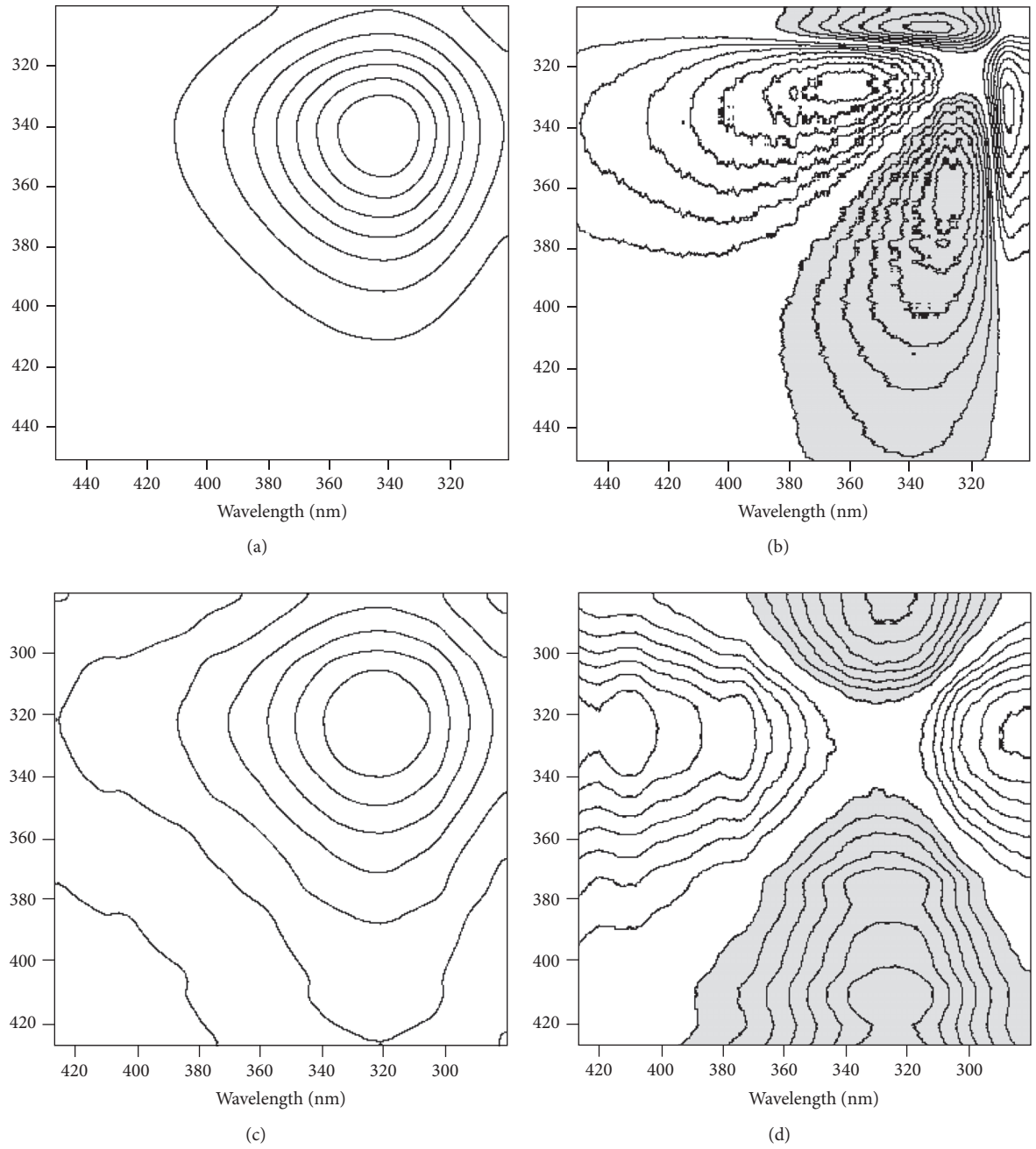

Figure 7: The synchronous and asynchronous 2D correlation fluorescence spectra of BSA solution (a, b) and BSA with CdTe/HA composites solution (c, d), constructed from the fluorescence spectra in Figure 8.

and emission wavelength of CdTe/HA composites. Besides, the fluorescence emission intensity of CdTe/HA composites can be enhanced by BSA, the mechanism of which was explained by FRET theory and two-dimensional correlation (2D COS) analysis. We believed that CdTe/HA composites did have a great potential in multicolor imaging and would be suitable for the further biological applications. But the binding mechanism between BSA and CdTe/HA composites and the application of this method in in vivo optical imaging are still unknown, and more in-depth researches should be adopted in the future.

Competing Interests

The authors declare that they do not have any commercial interest, financial interest, and/or other relationships with

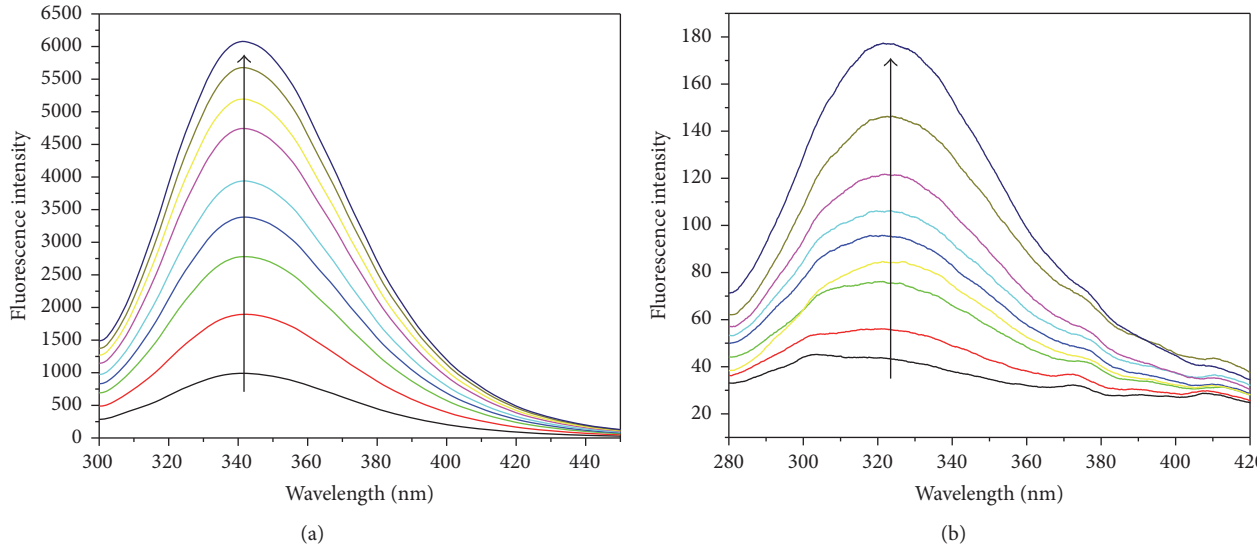

FIGURE 8: Fluorescence emission spectra of different concentrations of BSA solutions measured before (a) and after (b) addition to CdTe/HA composites solution (concentrations of BSA solutions from the bottom to the top are 0.05, 0.1, 0.15, 0.2, 0.25, 0.3, 0.35, 0.4, and 0.45 g/L) and an excitation wavelength of 280 nm was used for all samples.

manufacturers of pharmaceuticals, laboratory supplies, and/or medical devices or with commercial providers of medically related services.

Acknowledgments

The authors gratefully thank the National Natural Science Foundation of China (21405058, 21403087, 21401073, and 21375046) and Jilin Institute of Chemical Technology, China (no. 201341). They also gratefully thank Dr. Dayong Lu for the XRD analysis and Tao Zhou for the two-dimensional correlation (2D COS) analysis.

References

[1] M. Bruchez Jr., M. Moronne, P. Gin, S. Weiss, and A. P. Alivisatos, "Semiconductor nanocrystals as fluorescent biological labels," *Science*, vol. 281, no. 5385, pp. 2013–2016, 1998.

[2] X. Gao, Y. Cui, R. M. Levenson, L. W. K. Chung, and S. Nie, "In vivo cancer targeting and imaging with semiconductor quantum dots," *Nature Biotechnology*, vol. 22, no. 8, pp. 969–976, 2004.

[3] A. P. Alivisatos, "Semiconductor clusters, nanocrystals, and quantum dots," *Science*, vol. 271, no. 5251, pp. 933–937, 1996.

[4] Y. Cao, R. Jin, and C. A. Mirkin, "DNA-modified core-shell Ag/Au nanoparticles," *Journal of the American Chemical Society*, vol. 123, no. 32, pp. 7961–7962, 2001.

[5] X. H. Zhong, Y. Y. Feng, W. J. Knoll, and M. Han, "Alloyed $Zn_xCd_{1-x}S$ nanocrystals with highly narrow luminescence spectral width," *Journal of the American Chemical Society*, vol. 125, no. 44, pp. 13559–13563, 2003.

[6] S. Kim, Y. T. Lim, E. G. Soltesz et al., "Near-infrared fluorescent type II quantum dots for sentinel lymph node mapping," *Nature Biotechnology*, vol. 22, no. 1, pp. 93–97, 2004.

[7] E. Yaghini, A. M. Seifalian, and A. J. MacRobert, "Quantum dots and their potential biomedical applications in photosensitization for photodynamic therapy," *Nanomedicine*, vol. 4, no. 3, pp. 353–363, 2009.

[8] R. Freeman and I. Willner, "Optical molecular sensing with semiconductor quantum dots (QDs)," *Chemical Society Reviews*, vol. 41, no. 10, pp. 4067–4085, 2012.

[9] W.-P. Hu, G.-D. Cao, W. Dong, H.-B. Shen, X.-H. Liu, and L.-S. Li, "Interaction of quercetin with aqueous CdSe/ZnS quantum dots and the possible fluorescence probes for flavonoids," *Analytical Methods*, vol. 6, no. 5, pp. 1442–1447, 2014.

[10] N. N. Mamedova, N. A. Kotov, A. L. Rogach, and J. Studer, "Albumin-CdTe nanoparticle bioconjugates: preparation, structure, and interunit energy transfer with antenna effect," *Nano Letters*, vol. 1, no. 6, pp. 281–286, 2001.

[11] C. R. Patra, R. Bhattacharya, S. Patra, S. Basu, P. Mukherjee, and D. J. J. Mukhopadhyay, "Inorganic phosphate nanorods are a novel fluorescent label in cell biology," *Journal of Nanobiotechnology*, vol. 4, article 11, 2006.

[12] S. V. Dorozhkin and M. Epple, "Biological and medical significance of calcium phosphates," *Angewandte Chemie—International Edition*, vol. 41, no. 17, pp. 3130–3146, 2002.

[13] L. C. Palmer, C. J. Newcomb, S. R. Kaltz, E. D. Spoerke, and S. I. Stupp, "Biomimetic systems for hydroxyapatite mineralization inspired by bone and enamel," *Chemical Reviews*, vol. 108, no. 11, pp. 4754–4783, 2008.

[14] J. M. Sautier, J. R. Nefussi, and N. Forest, "Surface-reactive biomaterials in osteoblast cultures: an ultrastructural study," *Biomaterials*, vol. 13, no. 6, pp. 400–402, 1992.

[15] L. L. Hench, "Bioceramics: from concept to clinic," *Journal of the American Ceramic Society*, vol. 74, no. 7, pp. 1487–1510, 1991.

[16] A. C. Queiroz, J. D. Santos, and F. J. Monteiro, "Porous HA scaffolds for drug releasing," *Key Engineering Materials*, vol. 284–286, pp. 407–410, 2005.

[17] A. Tabaković, M. Kester, and J. H. Adair, "Calcium phosphate-based composite nanoparticles in bioimaging and therapeutic

delivery applications," *Wiley Interdisciplinary Reviews: Nanomedicine and Nanobiotechnology*, vol. 4, no. 1, pp. 96–112, 2012.

[18] P. Yang, Z. Quan, C. Li, X. Kang, H. Lian, and J. Lin, "Bioactive, luminescent and mesoporous europium-doped hydroxyapatite as a drug carrier," *Biomaterials*, vol. 29, no. 32, pp. 4341–4347, 2008.

[19] M. Kester, Y. Heakal, T. Fox et al., "Calcium phosphate nanocomposite particles for in vitro imaging and encapsulated chemotherapeutic drug delivery to cancer Cells," *Nano Letters*, vol. 8, no. 12, pp. 4116–4121, 2008.

[20] T. T. Morgan, H. S. Muddana, E. I. Altinoglu et al., "Encapsulation of organic molecules in calcium phosphate nanocomposite particles for intracellular imaging and drug delivery," *Nano Letters*, vol. 8, no. 12, pp. 4108–4115, 2008.

[21] Z. Y. Hou, P. P. Yang, H. Z. Lian et al., "Multifunctional hydroxyapatite nanofibers and microbelts as drug carriers," *Chemistry*, vol. 15, no. 28, pp. 6973–6982, 2009.

[22] P. Yang, S. Gai, and J. Lin, "Functionalized mesoporous silica materials for controlled drug delivery," *Chemical Society Reviews*, vol. 41, no. 9, pp. 3679–3698, 2012.

[23] R. J. Wiglusz, A. Bednarkiewicz, and W. J. Strek, "Synthesis and optical properties of Eu^{3+} ion doped nanocrystalline hydroxya patites embedded in PMMA matrix," *Journal of Rare Earths*, vol. 29, no. 12, pp. 1111–1116, 2011.

[24] D. E. Wagner, K. M. Eisenmann, A. L. Nestor-Kalinoski, and S. B. Bhaduri, "A microwave-assisted solution combustion synthesis to produce europium-doped calcium phosphate nanowhiskers for bioimaging applications," *Acta Biomaterialia*, vol. 9, no. 9, pp. 8422–8432, 2013.

[25] O. A. Graeve, R. Kanakala, A. Madadi, B. C. Williams, and K. C. Glass, "Luminescence variations in hydroxyapatites doped with Eu2+ and Eu3+ ions," *Biomaterials*, vol. 31, no. 15, pp. 4259–4267, 2010.

[26] Y. Lu, W. Yang, and M. Yin, "Comparative investigation on the crystal structure and cell behavior of rare-earth doped fluorescent apatite nanocrystals," *Materials Letters* , vol. 125, pp. 78–81, 2014.

[27] A. Z. Alshemary, M. Akram, Y.-F. Goh, M. R. Abdul Kadir, A. Abdolahi, and R. Hussain, "Structural characterization, optical properties and in vitro bioactivity of mesoporous erbium-doped hydroxyapatite," *Journal of Alloys and Compounds*, vol. 645, pp. 478–486, 2015.

[28] G. Jiang, K. Park, J. Kim, K. S. Kim, and S. K. Hahn, "Target specific intracellular delivery of siRNA/PEI–HA complex by receptor mediated endocytosis," *Molecular Pharmaceutics*, vol. 6, no. 3, pp. 727–737, 2009.

[29] P. F. Li, A. H. Yao, T. Zhou, and D. P. Wang, "Fabrication of N-acetyl-l-cysteine-capped CdSe-polyelectrolytes @ hydroxyapatite composite microspheres for fluorescence detection of Cu^{2+} ions," *Journal of Materials Science & Technology*, vol. 29, no. 11, pp. 1104–1110, 2013.

[30] A. H. Gore, M. B. Kale, P. V. Anbhule, S. R. Patil, and G. B. Kolekar, "A novel FRET probe for selective and sensitive determination of vitamin B_{12} by functionalized CdS QDs in aqueous media: applications to pharmaceutical and biomedical analysis," *RSC Advances*, vol. 4, no. 2, pp. 683–692, 2014.

[31] M.-H. Sorouraddin, A. Imani-Nabiyyi, S. A. Najibi-Gehraz, and M.-R. Rashidi, "A new fluorimetric method for determination of valproic acid using TGA-capped CdTe quantum dots as proton sensor," *Journal of Luminescence*, vol. 145, pp. 253–258, 2014.

[32] P. Dutta, D. Saikia, N. C. Adhikary, and N. S. Sarma, "Macromolecular systems with MSA-Capped CdTe and CdTe/ZnS Core/Shell quantum dots as superselective and ultrasensitive optical sensors for picric acid explosive," *ACS Applied Materials and Interfaces*, vol. 7, no. 44, pp. 24778–24790, 2015.

[33] S. Huang, F. Zhu, Q. Xiao et al., "A CdTe/CdS/ZnS core/shell/shell QDs-based 'oFF-ON' fluorescent biosensor for sensitive and specific determination of l-ascorbic acid," *RSC Advances*, vol. 4, no. 87, pp. 46751–46761, 2014.

[34] S. Zhuo, J. Gong, P. Zhang, and C. Zhu, "High-throughput and rapid fluorescent visualization sensor of urinary citrate by CdTe quantum dots," *Talanta*, vol. 141, pp. 21–25, 2015.

[35] F. Shi, Y. Li, Z. Lin, D. Ma, and X. Su, "A novel fluorescent probe for adenosine 5′-triphosphate detection based on Zn^{2+}-modulated l-cysteine capped CdTe quantum dots," *Sensors and Actuators, B: Chemical*, vol. 220, pp. 433–440, 2015.

[36] M. A. Correa-Duarte, M. Giersig, and L. M. Liz-Marzán, "Stabilization of CdS semiconductor nanoparticles against photodegradation by a silica coating procedure," *Chemical Physics Letters*, vol. 286, no. 5-6, pp. 497–501, 1998.

[37] T. Nann and P. Mulvaney, "Einzelne Quantenpunkte in Siliciumdioxid-Kugeln," *Angewandte Chemie*, vol. 116, no. 40, pp. 5511–5514, 2004.

[38] T. Nann and P. Mulvaney, "Single quantum dots in spherical silica particles," *Angewandte Chemie*, vol. 43, no. 40, pp. 5393–5396, 2004.

[39] W. W. Yu and X. Peng, "Formation of high-quality CdS and other II–VI semiconductor nanocrystals in noncoordinating solvents: tunable reactivity of monomers," *Angewandte Chemie—International Edition*, vol. 41, no. 13, pp. 2368–2371, 2002.

[40] D. H. Yu, Z. Wang, Y. Liu et al., "Quantum dot-based pH probe for quick study of enzyme reaction kinetics," *Enzyme and Microbial Technology*, vol. 41, no. 1-2, pp. 127–132, 2007.

[41] Y. Yue, T.-Y. Liu, H.-W. Li, Z. Liu, and Y. Wu, "Microwave-assisted synthesis of BSA-protected small gold nanoclusters and their fluorescence-enhanced sensing of silver(I) ions," *Nanoscale*, vol. 4, no. 7, pp. 2251–2254, 2012.

[42] International Conference on Harmonization (ICH) of Technical Requirements for Registration of Pharmaceuticals for Human Use, Topic Q2 (R1): Validation of Analytical Procedures: Text and Methodology, 2005, http://www.ich.org.

[43] J. R. Lakowicz, *Principles of Fluorescence Spectroscopy*, Springer, New York, NY, USA, 3rd edition, 2006.

[44] A. Sułkowska, "Interaction of drugs with bovine and human serum albumin," *Journal of Molecular Structure*, vol. 614, no. 1–3, pp. 227–232, 2002.

[45] X. M. He and D. C. Carter, "Atomic structure and chemistry of human serum albumin," *Nature*, vol. 358, no. 6383, pp. 209–215, 1992.

[46] X. L. Cao, H. W. Li, L. L. Lian, N. Xu, D. W. Lou, and Y. Wu, "A dual-responsive fluorescence method for the detection of clenbuterol based on BSA-protected gold nanoclusters," *Analytica Chimica Acta*, vol. 871, pp. 43–50, 2015.

[47] J. B. A. Ross, C. J. Schmidt, and L. Brand, "Time-resolved fluorescence of the two tryptophans in horse liver alcohol dehydrogenase," *Biochemistry*, vol. 20, no. 15, pp. 4369–4377, 1981.